Swarthmore College
Works

Chemistry & Biochemistry Faculty Works | Chemistry & Biochemistry

11-21-2006

Rovibrational Resonance Effects In Collision-Induced Electronic Energy Transfer: I2(E,v=0-2)+CF4

J. M. Hutchison

Benjamin Robert Booth Carlisle , '05

Thomas Alex Stephenson
Swarthmore College, tstephe1@swarthmore.edu

Follow this and additional works at: http://works.swarthmore.edu/fac-chemistry

 Part of the Physical Chemistry Commons

Recommended Citation

J. M. Hutchison; Benjamin Robert Booth Carlisle , '05; and Thomas Alex Stephenson. (2006). "Rovibrational Resonance Effects In Collision-Induced Electronic Energy Transfer: I2(E,v=0-2)+CF4". *Journal Of Chemical Physics*. Volume 125, Issue 19.
http://works.swarthmore.edu/fac-chemistry/14

This Article is brought to you for free and open access by the Chemistry & Biochemistry at Works. It has been accepted for inclusion in Chemistry & Biochemistry Faculty Works by an authorized administrator of Works. For more information, please contact myworks@swarthmore.edu.

Rovibrational resonance effects in collision-induced electronic energy transfer: I 2 (E , v = 0 – 2) + C F 4

J. Matthew Hutchison, Benjamin R. Carlisle, and Thomas A. Stephenson

Citation: The Journal of Chemical Physics **125**, 194313 (2006); doi: 10.1063/1.2363985
View online: http://dx.doi.org/10.1063/1.2363985
View Table of Contents: http://scitation.aip.org/content/aip/journal/jcp/125/19?ver=pdfcov
Published by the AIP Publishing

This article is copyrighted as indicated in the abstract. Reuse of AIP content is subject to the terms at: http://scitation.aip.org/termsconditions. Downloaded to IP: 130.58.65.10 On: Wed, 27 Nov 2013 21:36:19

Rovibrational resonance effects in collision-induced electronic energy transfer: $I_2(E, v=0-2)+CF_4$

J. Matthew Hutchison, Benjamin R. Carlisle,[a] and Thomas A. Stephenson[b]
Department of Chemistry and Biochemistry, Swarthmore College, Swarthmore, Pennsylvania 19081

(Received 30 August 2006; accepted 21 September 2006; published online 17 November 2006)

Collisions of I_2 in the $E(0_g^+)$ electronic state with CF_4 molecules induce electronic energy transfer to the nearby D, β, and D' ion-pair states. Simulations of dispersed fluorescence spectra reveal collision-induced electronic energy transfer rate constants and final vibrational state distributions within each final electronic state. In comparison with earlier reports on $I_2(v_E=0-2)$ collisions with He or Ar atoms, we find markedly different dynamics when I_2, excited to the same rovibronic states, collides with CF_4. Final vibrational state distributions agree with the associated Franck-Condon factors with the initially prepared state to a greater degree than those found with He or Ar collision partners and suggest that internal degrees of freedom in the CF_4 molecule represent a substantial means for accepting the accompanying loss of I_2 vibronic energy. Comparison of the $E \rightarrow D$ transfer of I_2 excited to the $J=23$ and $J=55$ levels of the $v_E=0$ state reveals the onset of specific, nonstatistical dynamics as the available energy is increased above the threshold for excitation of the low frequency ν_2 bending mode of CF_4. © *2006 American Institute of Physics*.
[DOI: 10.1063/1.2363985]

I. INTRODUCTION

Over the past decade a number of studies have demonstrated the rich electronic energy transfer dynamics that accompany collisions of diatomic iodine prepared in an ion-pair electronic state with atomic, diatomic, and polyatomic collision partners.[1–13] The initial work in this field was reported by Ubachs *et al.*[1] and Teule *et al.*,[2] and considered collisions of ion-pair state excited I_2 with $I_2(X)$. More recently, reports from this laboratory[3–5] and the experiments of Pravilov and co-workers[6–9] have focused on studies involving a variety of collision partners interacting with I_2 prepared in the $E(0_g^+)$ electronic state in one of a range of initial vibrational levels. These studies fall into two general categories: Pravilov and co-workers have examined the collision-induced electronic energy transfer dynamics that result from collisions of I_2 prepared in high vibrational levels ($v=8-47$) of the E electronic state[6–9] [or most recently, a range of vibrational levels in the higher energy $f(0_g^+)$ ion-pair state[10,11]] with the collision partners He, Ar, $I_2(X)$, N_2, and CF_4. In this laboratory, our focus has been on preparing low vibrational levels of the E electronic state and using a narrower range of collision partners—$I_2(X)$ and rare gas atoms.[3–5]

In Fig. 1, the potential energy curves for the lowest energy region of the so-called first tier of ion-pair states in I_2 are displayed. These states all correlate with the separated ion limit $I^+(^3P_2)+I^-(^1S_0)$ and are characterized by a large dissociation energy ($\approx$31 000 cm^{-1}).[14] Note that a total of six ion-pair states exists with T_e values that lie within 1500 cm^{-1} of one another. For these first-tier states, ease of experimental preparation in double resonance experiments ($E \leftarrow B \leftarrow X$) has focused the previous laboratory experiments exclusively on the collision dynamics that result following excitation of the E ion-pair state.[3–9,12] All of these previous investigations reveal the importance of $E \rightarrow D$ collision-induced electronic energy transfer.[12] Experiments in this laboratory have also demonstrated the presence of both $E \rightarrow D'$ and $E \rightarrow \beta$ energy transfer following excitation of I_2 to low vibrational levels in the E state when He or Ar is the collision partner.[3,5] The major focus of all the investigations—at both high and low levels of vibrational excitation in the E state—has been on gaining a complete understanding of the propensity rules that govern the distribution of vibrational energy in the final electronic state(s).

Comparison of these studies reveals that increasing the vibrational energy in the E electronic state not only increases the overall cross section for electronic energy transfer but also alters the trends in the propensity rules for collision-induced vibrational populations. For example, for rare gas collision partners, at low vibrational energies ($v_E=0-2$), Franck-Condon factors compete with energy gap effects in determining the D state vibrational distributions.[3,5] At higher vibrational levels, the general trend is that energy gap effects are dominant, with the D state vibrational distributions having an almost symmetric appearance centered at a D state vibrational level that is nearly resonant with the initially prepared E state level.[6,8–10] This variation in behavior with initial vibrational level is attributed to a significant broadening of the distribution of Franck-Condon factors between E and D state vibrational levels at high values of v_E.[12] Thus, significant impediments to the population of near resonant levels due to very unfavorable vibrational wave function overlaps are removed at high values of v_E.

As noted previously, Pravilov and co-workers extended

[a]Present address: Cornell University Law School, Ithaca, NY 14853.
[b]Electronic mail: tstephe1@swarthmore.edu

 © 2006 American Institute of Physics

This article is copyrighted as indicated in the abstract. Reuse of AIP content is subject to the terms at: http://scitation.aip.org/termsconditions. Downloaded to IP: 130.58.65.10 On: Wed, 27 Nov 2013 21:36:19

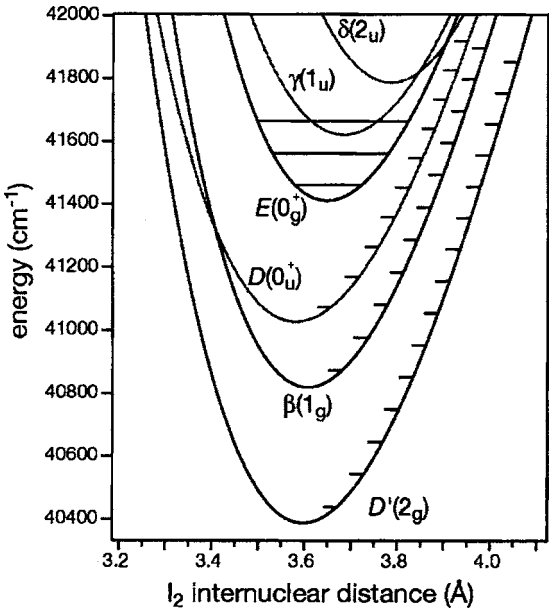

FIG. 1. The first tier of ion-pair states in I_2. Energy on the vertical axis is relative to T_e of the ground $X(^1\Sigma_g^+)$ state. Vibrational levels are indicated by tick marks at the outer turning point of the three lowest energy states. The three vibrational levels of the $E(0_g^+)$ state we access in the experiment are shown as full lines.

their work on the collision dynamics of high vibrational levels of the E state by examining collisions with a polyatomic molecule, CF_4.[6,9] The distribution of population in the vibrational levels in the D electronic state that results from electronic energy transfer was found to be multimodal. Significant population was found in the D state levels that are near resonant with the initially prepared E state level, just as observed for rare gas collision partners. Unique to the case of CF_4 collisions, however, was the observation of population in D state levels with energy gaps that coincided with the vibrational frequencies of ground electronic state CF_4. These results are consistent with a model in which vibrational excitation of the CF_4 serves to minimize the amount of I_2 vibronic energy released to relative translation of the recoiling species. A similar mechanism was implicated in early work on electronic energy transfer in collisions of $I_2(E)$ and $I_2(X)$.[2]

The intriguing observation of nearly resonant energy transfer into the CF_4 internal degrees of freedom provides the motivation for the work described in this manuscript. Our previous studies have demonstrated that collisions involving I_2 prepared in the lowest vibrational levels of the E state result in electronic energy transfer pathways that are distinct from those observed at higher vibrational energies.[3–5,12] At the same time, the relative simplicity of the spectroscopy of the ion-pair states for the lowest vibrational levels allows for a somewhat more detailed analysis of the processes observed. In the sections that follow, we present the results of our investigations that strongly suggest that resonant energy transfer into the energetically available vibrational states of CF_4 is a universal feature of the $I_2(E)+CF_4$ collision dynamics.

II. EXPERIMENT

Our experimental strategy has been used in previous work from our laboratory and is described in detail elsewhere.[3–5] Briefly, we prepare single rovibrational levels of the E ion-pair state of iodine through double resonance excitation. For all excitation schemes, a Nd^{3+}:YAG (yttrium aluminum garnet) pumped dye laser system (Continuum Lasers YG580/TDL-50, ~0.15 cm^{-1} bandwidth) provides light resonant with a $B \leftarrow X$ transition (λ_1), and a N_2-pumped dye laser system (Laser Photonics UV24/DL-14P, ~0.25 cm^{-1} bandwidth) provides light resonant with the corresponding $E \leftarrow B$ transition (λ_2). We prepare electronically excited iodine with 0, 1, or 2 quanta of vibrational excitation in either the $J_E=23$ or $J_E=55$ rotational level. Excitation schemes along with λ_1 and λ_2 values are shown in Table I.

Excitation of I_2 vapor occurs in a glass and fused silica cell, equipped with Brewster's angle laser inlet and exit windows. In the experiments reported, we use 40 mTorr I_2 vapor (Aldrich, 99.999%) and a variable pressure of CF_4 (Aldrich, 99.9%), typically 200–1000 mTorr. Double resonance excitation results in intense $E \rightarrow B$ emission between 415 and 435 nm, as well as a number of weaker features, depending on the sample pressure conditions. We measure I_2 fluorescence after dispersion through a 0.5 m focal length scanning monochromator (Instruments SA 500M). The exit slit of the monochromator has been replaced with a charge-coupled device (CCD) camera (Princeton Instruments LN/CCD-2500PB); we record a total spectral width of ~24 nm in a single exposure.

We simulate the dispersed fluorescence spectra to extract the distribution of electronic and vibrational states populated through collision-induced electronic energy transfer. Spectroscopic constants were taken from the literature for the electronic ground state $X(0_g^+)$,[15] excited valence states $A'(2_u)$,[16] $A(1_u)$,[17] and $B(0_u^+)$,[18] and ion-pair states $D'(2_g)$,[19] $\beta(1_g)$,[20] $D(0_u^+)$,[21] and $E(0_g^+)$.[22] We calculate Franck-Condon factors through computer code based on the Numerov method,[23] which calculates numerical wave functions for a given one-

TABLE I. Excitation schemes and wavelengths used for the preparation of electronically excited ion-pair states of I_2.

E state		$B \leftarrow X$			$E \leftarrow B$		
v_E	J_E	(v_B, v_X)	$\Delta J(J_X)$	λ_1 (nm)	(v_E, v_B)	$\Delta J(J_B)$	λ_2 (nm)
0	23	(20, 0)	$R(23)$	559.05	(0, 20)	$P(24)$	426.29
0	55	(20, 0)	$R(55)$	559.95	(0, 20)	$P(56)$	426.56
1	55	(21, 0)	$R(55)$	557.18	(1, 21)	$P(56)$	426.34
2	55	(21, 0)	$R(55)$	557.18	(2, 21)	$P(56)$	424.53

This article is copyrighted as indicated in the abstract. Reuse of AIP content is subject to the terms at: http://scitation.aip.org/termsconditions. Downloaded to IP: 130.58.65.10 On: Wed, 27 Nov 2013 21:36:19

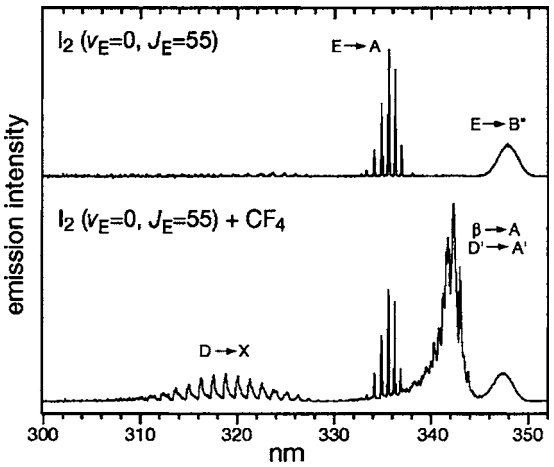

FIG. 2. Dispersed fluorescence spectra of I_2 obtained after excitation to the state ($v_E=0$, $J_E=55$). Spectral features include emission from the vibrational state we prepare, dominant in the sample of pure I_2 vapor (top half), and from electronic states populated through collisions with CF_4 (bottom half).

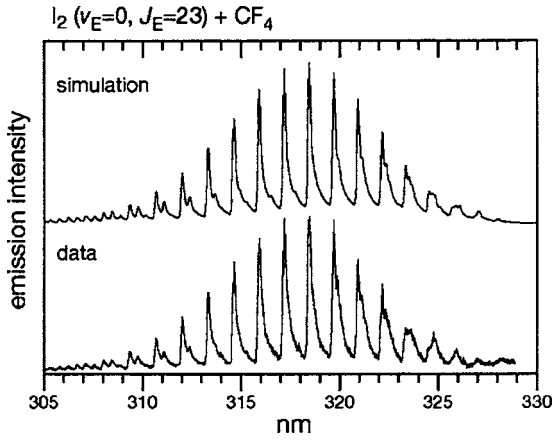

FIG. 3. $D\rightarrow X$ emission after collision-induced electronic energy transfer of $I_2(v_E=0, J_E=23)$ by CF_4. The simulated spectrum (top) uses only our statistical model for determining the D state rotational level population and accurately reproduces the experimental spectrum (bottom).

dimensional potential. Rydberg-Klein-Rees potential energy curves were taken directly from the literature for the A', D', D, and E states[16,19,21,22] and calculated from spectroscopic constants[24] for the X, A, and β states.[15,17,20]

III. RESULTS AND DISCUSSION

Dispersed fluorescence of I_2 after excitation to the E ion-pair state shows intense $E\rightarrow B$ transitions along with weaker $E\rightarrow A$ and $E\rightarrow B''(1_u)$ bands.[3–5,12] The top half of Fig. 2 shows the region of the fluorescence spectrum from 40 mTorr I_2 excited to the state ($v_E=0$, $J_E=55$) including the $E\rightarrow A$ (332–338 nm) and $E\rightarrow B''$ (345–351 nm) spectral features. There are additional weak features between 300 and 330 nm assigned to $D\rightarrow X$ emission. Here, the D state is populated through collisions with ground state iodine molecules, $I_2(E)+I_2(X)$.[4] In the following analysis of $E\rightarrow D$ energy transfer through collisions of I_2 with CF_4, we have subtracted the relatively weak $D\rightarrow X$ emission seen here for a sample of pure I_2.

In similar behavior to collisions with He and Ar,[3] collisions with CF_4 induce transitions in $I_2(E)$ to the lower energy ion-pair states D', β, and D. Upon addition of CF_4 gas to our sample cell, fluorescence due to collision-induced energy transfer dominates the emission spectrum between 300 and 350 nm. The bottom half of Fig. 2 shows the fluorescence spectrum from a cell filled with 40 mTorr I_2 and 250 mTorr CF_4 in which the I_2 has been excited to the state ($v_E=0$, $J_E=55$). As indicated in Fig. 2, the spectral features of interest include $D(0_u^+)\rightarrow X(0_g^+)$ emission between 305 and 330 nm and the overlapping $\beta(1_g)\rightarrow A(1_u)$ and $D'(2_g)\rightarrow A'(2_u)$ emissions between 334 and 346 nm. We find the fluorescence intensity from the ion-pair states D', β, and D to be linear with the pressure of CF_4 for all experiments described herein, indicative of single collision conditions.

Collisions of I_2 in low vibrational levels of the E state with CF_4 molecules induce transitions into a range of vibrational and rotational levels in the D, β, and D' electronic ion-pair states. To extract the distribution of vibrational levels populated through collision-induced energy transfer in a given electronic state, we perform spectral simulations of the fluorescence spectra, where the populations of the $v=0-7$ vibrational levels in the given electronic state are variable parameters.

A. $E\rightarrow D$ transfer

1. $v_E=0$, $J_E=23$

The $D\rightarrow X$ emission recorded after excitation to the ($v_E=0$, $J_E=23$) level of a 40 mTorr I_2 sample with 517 mTorr CF_4 is shown in the bottom half of Fig. 3, where each peak in this spectrum corresponds to a particular vibronic transition. Each peak is slightly asymmetric with a more gradual tail toward the long-wavelength side. We attribute the asymmetry of these peaks to rotational relaxation that accompanies the collision-induced electronic energy transfer process. As we are unable to resolve the rotational fine structure in our fluorescence spectra, our bands appear asymmetric, where fluorescence from states with J_D larger than the initial J_E occurs at longer wavelengths than the peak transition.

To describe the rotational population of the D, β, and D' states in our fluorescence spectrum simulations, we use a statistical exponential-power gap model that is frequently used for collision-induced rotational relaxation,[25]

$$P(J_f)\propto\frac{(2J_<+1)}{(2J_i+1)}\left(\frac{\Delta E_{\rm rot}}{B_v}\right)^{-\alpha}\exp(-\theta\Delta E_{\rm rot}).$$

$P(J_f)$ is the probability of transfer to the rotational state J_f, J_i is the rotational state populated in the absence of rotational relaxation, $J_<$ is the smaller of J_f and J_i, B_v is the rotational constant for the vibrational state in question, and $\Delta E_{\rm rot}$ is the difference in energy between the states J_f and J_i. The parameters α and θ are adjusted to best match the experimental spectrum. Because the $E\rightarrow D$ transfer involves a $g\rightarrow u$ change of inversion symmetry in the electronic wave function, conservation of nuclear spin symmetry dictates that only even values of J_D are populated in the D state when an odd value of J_E is prepared in the E state. Correspondingly, we assume that the $J_D=22$ or $J_D=54$ rotational level is popu-

This article is copyrighted as indicated in the abstract. Reuse of AIP content is subject to the terms at: http://scitation.aip.org/termsconditions. Downloaded to IP: 130.58.65.10 On: Wed, 27 Nov 2013 21:36:19

TABLE II. Probability distribution of transfer to specific vibrational levels of the D ion-pair state, $P(v_D)$. Data are shown for two different initially prepared rotational states of $v_E=0$. Numbers in parentheses are one standard deviation in units of the last digit reported. Franck-Condon factors between the states ($v_E=0$, $J_E=23$) and (v_D, $J_D=22$) are given, with those less than 10^{-3} listed as zero.

v_D	($v_E=0$, $J_E=23$) $P(v_D)$	($v_E=0$, $J_E=55$) $P(v_D)$	Franck-Condon factor
0	0.766 (5)	0.695 (23)	0.659
1	0.137 (9)	0.187 (13)	0.297
2	0.051 (6)	0.068 (18)	0.042
3	0.017 (6)	0.022 (5)	0.002
4	0.001 (2)	0.004 (2)	0
5	0.018 (7)	0.000 (1)	0
6	0.010 (3)	0.022 (9)	0
7	0.000 (1)	0.001 (1)	0

lated in the D state in the absence of rotational relaxation when we prepare $J_E=23$ or $J_E=55$, respectively.

We find the vibrational distributions in the D, β, and D' states discussed below to be relatively insensitive to the values of α and θ, and use $\alpha=0.6$ and $\theta=0.002$ cm for all vibrational levels in all of our simulations. These values are in no way unique—we do not have the resolution to definitively comment on the relative accuracy of this statistical rotational energy redistribution. We simply find this model to be useful in accounting for the innate asymmetry of our spectral bands.

Our simulation of the $D \rightarrow X$ emission following excitation to ($v_E=0$, $J_E=23$) is shown in the top half of Fig. 3 and faithfully reproduces all spectral features and band shapes. The population distribution of D state vibrational levels, $P(v_D)$, averaged over spectra obtained with six different pressures of CF_4, is shown in Table II. These data show a clear preference for the population of $v_D=0$. Of the collisions with CF_4 that induce transfer to the D state, over 75% of them cause transfer to the ground vibrational level. Indeed, the trend in transfer probability for the first eight vibrational levels of the D state reflects the trend in Franck-Condon factors between each v_D and the initially prepared state ($v_E=0$, $J_E=23$), as listed in Table II. This is a markedly different trend in $P(v_D)$ than that previously reported from our laboratory on collisions of $I_2(v_E=0)$ with He or Ar atoms,[3] in which the trend was best described as a balance between pathways that maximized Franck-Condon overlap of the initial and final vibrational wave functions and those that also minimized the energy gap.

2. $v_E=0$, $J_E=55$

Following excitation of a 40 mTorr I_2 and 1004 mTorr CF_4 sample to the state ($v_E=0$, $J_E=55$), a rotational level ~ 50 cm^{-1} higher in energy than ($v_E=0$, $J_E=23$), we observe a $D \rightarrow X$ emission that is superficially very similar to that shown in Fig. 3. Consistent with this result, the D state vibrational distributions following excitation of ($v_E=0$, $J_E=23$) and ($v_E=0$, $J_E=55$) are roughly the same (Table II). We observe, however, that each $D \rightarrow X$ vibronic transition has a substantially increased spectral width following excitation of ($v_E=0$, $J_E=55$). We attribute this width to a larger distribution of rotational states that accompanies the collision-induced electronic energy transfer.

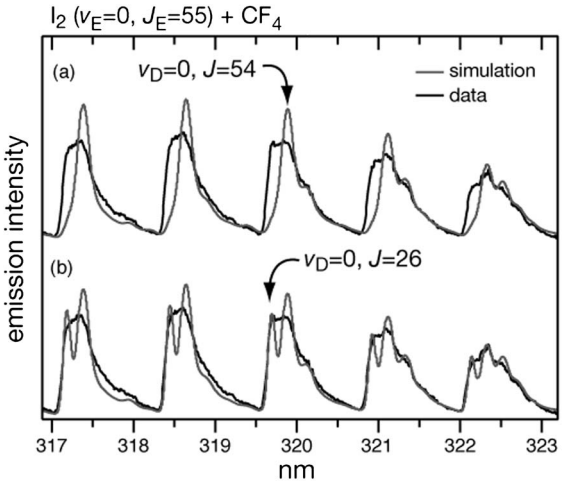

FIG. 4. Detail of the experimental spectrum (black) that results from excitation of a 40 mTorr I_2 and 1004 mTorr CF_4 sample to the state ($v_E=0$, $J_E=55$), overlaid with two spectral simulations (gray). (a) The rotational level distribution of the simulation is solely given by our statistical function. (b) Additional emission from the state ($v_D=0$, $J_D=26$) is added to the simulation in part (a) which accounts for the short-wavelength side of each peak.

Our best fit using the statistical exponential-power gap model to simulate this emission spectrum reproduces the overall intensities of the $D \rightarrow X$ transitions, but as shown in Fig. 4(a), the width of each vibronic transition in the experimental spectrum is considerably larger than that produced by our rotational relaxation model. Adjusting the values of α, θ, or J_i does not significantly improve the quality of our fit. Here we see that our statistical function for the rotational distribution does a good job of recovering the long-wavelength, or high J_D, side of each vibronic transition. It is only those peaks corresponding to emission from $v_D=0$ that contain additional low J (short-wavelength) emission intensity. We interpret the short-wavelength intensity to be a signature of additional nonstatistical dynamics in the collision-induced electronic energy transfer that specifically populates low J rotational levels of the $v_D=0$ vibrational level, dynamics that are absent in transfer from ($v_E=0$, $J_E=23$).

Following the results of $I_2(v_E=8-47)+CF_4$ collision-induced electronic energy transfer experiments by Pravilov and co-workers,[6,9] we interpret our results as a resonant excitation of CF_4 vibrational modes to explain these anomalous nonstatistical dynamics. An energy level diagram of the relevant rotational levels of $v_D=0$ and $v_E=0$ in I_2, including energy differences (cm^{-1}), is shown in Fig. 5. Because the rotational constants for the $v=0$ levels of the D and E states do not differ significantly, the energy gaps for energy transfer pathways that minimize $\Delta J(J_E-J_D)$ are relatively independent of J_E and are equal to ~ 389 cm^{-1}. Conversely, the transitions that involve that largest possible loss in iodine rovibronic energy, i.e., those terminating at ($v_D=0$, $J_D=0$), are significantly different: 399.5 cm^{-1} from ($v_E=0$, $J_E=23$) and 449.8 cm^{-1} from ($v_E=0$, $J_E=55$).

The lowest energy vibrational frequency of CF_4 is the ν_2 bending mode at 435.399 cm^{-1}.[26] Therefore, in the $v_E=0$

This article is copyrighted as indicated in the abstract. Reuse of AIP content is subject to the terms at: http://scitation.aip.org/termsconditions. Downloaded to IP: 130.58.65.10 On: Wed, 27 Nov 2013 21:36:19

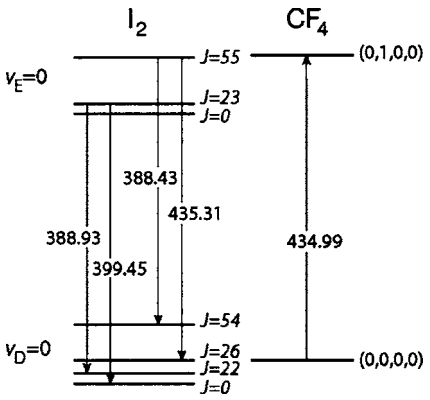

FIG. 5. Energy level diagram of selected rotational states of the $v_D=0$ and $v_E=0$ levels in I_2. Energy gaps (in cm^{-1}) show that the $(v_E=0,J_E=55)\rightarrow(v_D=0,J_D=26)$ transition is nearly resonant with the CF_4 bend fundamental (0,1,0,0), while there is insufficient available energy in transitions originating from $(v_E=0, J_E=23)$.

$\rightarrow v_D=0$ energy transfer channel, there is sufficient available energy in the $J_E=55$ experiment to selectively excite the ν_2 mode of CF_4 (assuming a large value of ΔJ), while there is an insufficient amount in the $J_E=23$ experiment. As shown in Fig. 5, it is the $(v_E=0,J_E=55)\rightarrow(v_D=0,J_D=26)$ energy transfer channel of I_2 that has an energy gap that is closest to the excitation energy of ν_2 in CF_4, $(0,1,0,0)\leftarrow(0,0,0,0)$. Figure 5 shows an energy difference of 434.99 cm^{-1}, corresponding to excitation of CF_4 with $J=30$, the most populated rotational level at room temperature. The slight shift from the fundamental ν_2 energy originates from the difference in rotational constants in the ground and excited ν_2 states of CF_4.[26]

To test this resonant nonstatistical model, we add additional fluorescence from the state $(v_D=0, J_D=26)$ in our $D\rightarrow X$ emission simulation. The results of our best fit are shown in Fig. 4(b). As can be clearly seen, emission from $(v_D=0, J_D=26)$ exactly matches the rise of the short-wavelength side of each peak corresponding to transitions from $v_D=0$. We surmise that this extra intensity is evidence of selective $E\rightarrow D$ energy transfer that is resonant with excitation of the lowest energy vibrational level in CF_4. This channel is absent in energy transfer from $(v_E=0, J_E=23)$ because of insufficient available energy. Averaged over six different CF_4 pressures, the intensity of the emission from $(v_D=0, J_D=26)$ represents $10\pm1\%$ of the total emission intensity. The values for $P(v_D)$ listed in Table II are only for the portion of the $D\rightarrow X$ emission from rotational states populated through the statistical mechanism.

In the interest of simplicity to our resonant energy transfer model, we have not considered energy transfer to other rotational states near $J_D=26$ that may also be populated in the nonstatistical energy transfer. This simplification manifests itself in our simulation, as seen in Fig. 4(b). There is a clear gap in the simulation between peaks from $(v_D=0, J_D=26)$ and peaks from the statistical rotational distribution centered at $(v_D=0, J_D=54)$ that does not adequately represent the experimental spectrum. A more sophisticated fitting routine could better fit the experimental spectrum by including additional fluorescence from J_D states between 26 and 54 that would fill in this gap. Transitions to such states in the

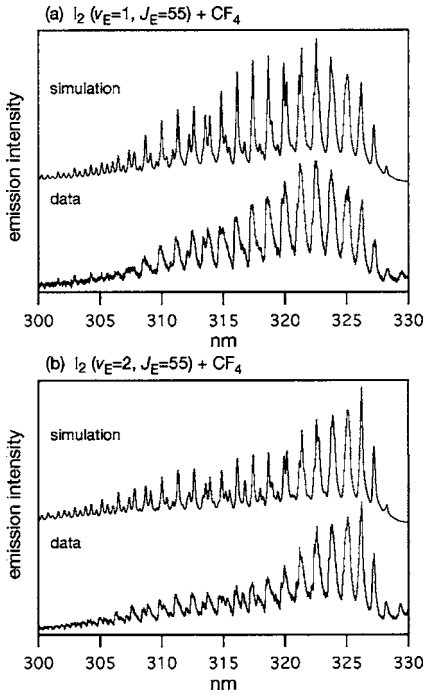

FIG. 6. $D\rightarrow X$ emission after collision-induced electronic energy transfer of (a) $I_2(v_E=1,J_E=55)$ and (b) $(v_E=2, J_E=55)$. The simulations only use the statistical function to model the D state rotational distribution.

electronic energy transfer process could be resonant, for example, with ν_2 transitions in CF_4 that are accompanied by a substantial change in CF_4 rotational energy. Additionally, due to our limited resolution, the rising edge on the low wavelength side of each $v_D=0$ peak can also be fitted by transitions from $J_D=22$ though $J_D=30$. However, we still use only $J_D=26$ to describe this low wavelength side because the $(v_E=0,J_E=55)\rightarrow(v_D=0,J_E=26)$ transition is the closest energy match to the $(0,1,0,0)J=30\leftarrow(0,0,0,0)J=30$ transition in CF_4.

3. $v_E=1-2$, $J_E=55$

In Fig. 6 we show emission spectra from samples of 40 mTorr I_2+1000 mTorr CF_4 excited to the states $(v_E=1, J_E=55)$ and $(v_E=2, J_E=55)$. Simulations using only the statistical function to describe the D state rotational distribution are also shown in Fig. 6, with the best fit vibrational state distributions $P(v_D)$ given in Table III. In a trend similar to the listed Franck-Condon factors and that reported in $I_2(v_E=0-2)$+He, Ar collisions, the $P(v_D)$ values for the $E\rightarrow D$ transfer are broadened and the maximum peaks at larger values of v_D as the initial level v_E is increased. However, in contrast to our previous work, the distributions in Table III peak at levels with a smaller v_D than those observed through collisions with He and Ar, a trend also shown above in transfer from $v_E=0$ (Table II).

The $P(v_D)$ distributions shown in Tables II and III all show a trend that is markedly different than those seen in collisions with He and Ar. The distribution of vibrational levels that are populated in the D state following collision with CF_4 is consistent to a greater extent with Franck-Condon factors with the initially prepared level than those observed after collision with He or Ar, the most extreme

This article is copyrighted as indicated in the abstract. Reuse of AIP content is subject to the terms at: http://scitation.aip.org/termsconditions. Downloaded to IP: 130.58.65.10 On: Wed, 27 Nov 2013 21:36:19

TABLE III. Probability distribution of transfer to specific vibrational levels of the D ion-pair state, $P(v_D)$. Data are shown for two different initially prepared vibrational levels with $J_E=55$. Numbers in parentheses are one standard deviation in units of the last digit reported. Franck-Condon factors (FCFs) between the states (v_E, $J_E=55$) and (v_D, $J_D=54$) are given, with those less than 10^{-3} listed as zero.

	($v_E=1$, $J_E=55$)		($v_E=2$, $J_E=55$)	
v_D	$P(v_D)$	FCF	$P(v_D)$	FCF
0	0.373 (26)	0.248	0.207 (19)	0.069
1	0.350 (14)	0.227	0.274 (35)	0.277
2	0.133 (5)	0.410	0.205 (24)	0.042
3	0.084 (20)	0.108	0.129 (17)	0.409
4	0.039 (11)	0.008	0.087 (36)	0.183
5	0.017 (18)	0	0.034 (23)	0.020
6	0.003 (3)	0	0.004 (8)	0
7	0.002 (5)	0	0.058 (10)	0

example seen in $v_E=0$. At the low levels of v_E investigated in our experiments, the v_D levels with the largest Franck-Condon factors with the initially prepared level correspond to energy gaps of 300–400 cm^{-1}. Because this energy difference must necessarily be transferred to translational energy upon collisions with He or Ar, any strong propensity for transfer to vibrational levels with a large vibrational wave function overlap is tempered by the need to transfer large amounts of energy into relative translation. The closer agreement of $P(v_D)$ trends with Franck-Condon factors upon collision with CF_4 indicates that there exists a propensity to populate vibrational levels with large wave function overlap in the $E \rightarrow D$ transfer and that the vibrational and rotational degrees of freedom in CF_4 are a more favorable acceptor of available energy than translation.

Comparison of the experimental and simulated $D \rightarrow X$ emission spectra in Fig. 6 shows similar behavior to that observed in emission after excitation to the state ($v_E=0$, $J_E=55$). Many peaks corresponding to emission from $v_D=0$ and $v_D=1$ have considerable intensity on the low wavelength side that is not reproduced with our statistical rotational distribution function. This effect is most easily seen in the difference in experiment and simulation between 310 and 320 nm, an area where emission from the two lowest energy vibrational states are prominent and well separated from emission from higher vibrational levels. Again, we interpret these wide spectral features to be evidence of specific rotational level energy transfer that is resonant with vibrational frequencies in CF_4. Unlike collisions with I_2 in the initial state ($v_E=0$, $J_E=55$) where there was only a maximum of ~450 cm^{-1} of available energy in the $E \rightarrow D$ transfer, there exists much more available energy in transfer from $v_E=1$ and $v_E=2$ to low vibrational levels of the D state. As a result, we are unable to make any unambiguous identifications of a specific I_2 rovibronic energy transfer channel that is resonant with a larger number of higher energy rovibrational transitions in CF_4. Better resolution of the rotational fine structure in the $D \rightarrow X$ emission could lead to a better understanding of the rotational distribution in the D state and, hence, a more complete picture of specific $E \rightarrow D$ channels resonantly enhanced through vibrational excitation of CF_4.

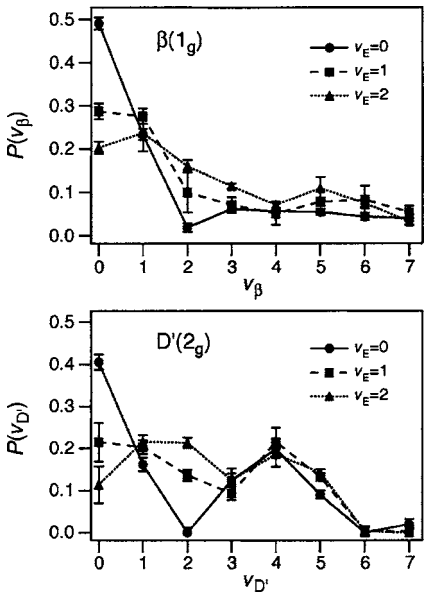

FIG. 7. Vibrational state distributions upon collision-induced electronic energy transfer to the β (top) and D' (bottom) electronic states from initial states ($v_E=0-2$, $J_E=55$).

B. $E \rightarrow D'$ and $E \rightarrow \beta$ transfer

Probability distributions for transfer to the lowest eight vibrational levels of the D' and β states are shown in Fig. 7. Because the $D' \rightarrow A'$ and $\beta \rightarrow A$ emissions from these states are overlapped between the wavelengths of 334 and 346 nm, we must fit the vibrational distribution from both states simultaneously.[3,5] In addition, we account for spectral bands due to the E state emission in the absence of collision-induced energy transfer (see Fig. 2). We find no significant rotational state dependence on the $E \rightarrow D'$ and $E \rightarrow \beta$ collision dynamics. Vibrational state distributions in the D' and β states are equal within our error bars after excitation to the initial states ($v_E=0$, $J_E=23$) and ($v_E=0$, $J_E=55$).

For all fits in this region, the statistical function for rotational state distribution adequately reproduces all of the spectral features. Thus, we see no direct evidence of any specific, nonstatistical, resonantly enhanced rovibronic energy transfer. However, given the complexity of this spectral region and our limited resolution, it is not surprising that we are unable to detect any subtle spectral features similar to those seen in the $D \rightarrow X$ emission after excitation to ($v_E=0-2$, $J_E=55$). As discussed below, the overall distribution of vibrational levels populated in both the D' and β states allows us to infer that CF_4 vibrational modes are a significant pathway to accept vibronic energy lost by I_2 in the energy transfer dynamics.

Again, the vibrational populations are markedly different than those produced in collisions with He or Ar.[3,5] Figure 7 shows a clear preference for transfer to vibrational levels with large Franck-Condon overlap—transitions that minimize the change in vibrational quantum number. Collisions with He and Ar produce much broader distributions with substantial probability to transfer population to states with a larger number of vibrational quanta than the initial v_E level—transitions with lower energy gaps than those with larger Franck-Condon factors. The D' and β states have signifi-

This article is copyrighted as indicated in the abstract. Reuse of AIP content is subject to the terms at: http://scitation.aip.org/termsconditions. Downloaded to IP: 130.58.65.10 On: Wed, 27 Nov 2013 21:36:19

cantly lower T_e values than the E state, and transitions that minimize the change in vibrational quantum number, i.e., have large Franck-Condon factors, correspond to changes of ~600 and ~1000 cm^{-1} in vibronic energy to the β and D' states, respectively. With He and Ar as the collision partner, transitions with a reduced energy gap are important in the collision dynamics. There is a reduced propensity for the population of states with large Franck-Condon overlap because of the impediment of transferring large amounts of energy into translation.

With CF_4 as a collision partner we observe a severe reduction of this impediment, as states with both large Franck-Condon factors and large energy gaps are populated in the electronic energy transfer. It is likely that the rotational and vibrational degrees of freedom in the CF_4 collision partner are effective at accepting the excess energy from the I_2 vibronic energy change. Because the magnitude of the energy gaps in these channels are on the order of 500–1000 cm^{-1}, we suggest that the two low frequency bending modes[26,27] of CF_4 at 435 and 631 cm^{-1} may be particularly effective in accepting excess energy at the low v_E levels reported here. The higher frequency stretching modes[27,28] at 909 and 1284 cm^{-1} may become important in accepting I_2 vibronic energy changes at higher values of v_E. Indeed, it is the v_3 bend at 631 cm^{-1} and ν_4 antisymmetric stretch at 1284 cm^{-1} that Pravilov and co-workers find to accept energy after collision-induced electronic energy transfer with $I_2(v_E=8-47)$.[6,9]

C. Kinetic analysis

We use the same kinetic analysis that was used for He and Ar collision partners to calculate collision-induced electronic energy transfer rate constants and hard-sphere collision cross sections. The scheme has been described previously in detail.[3,4] To determine the rate constant for the $E \rightarrow D$ transfer, for example, we find the ratio of the total intensity of the $D \rightarrow X$ emission to the $E \rightarrow B''$ emission. In previous work, we used the intensity of the $E \rightarrow A$ transitions rather than the $E \rightarrow B''$ intensity in the denominator of this ratio. As both of these transition intensities are linear with I_2 pressure and independent of CF_4 pressure, the results do not depend on which particular transitions we use to normalize the $D \rightarrow X$ intensities. However, because the $E \rightarrow A$ transitions are strongly overlapped by $D' \rightarrow A'$ and $\beta \rightarrow A$ emissions at high CF_4 pressures, we find less error in the ratio when the $E \rightarrow B''$ intensity is used. Confirmation that this ratio is linear with the pressure of CF_4 indicates that we are operating with single collision conditions. We use Einstein $A_{n,m}$ coefficients for the particular electronic transitions and the radiative lifetime of the E electronic state (25.7 ns) from the literature[29] to extract the energy transfer rate constants from the intensity ratio.

The second-order collision-induced electronic energy transfer rate constants and effective hard-sphere cross sections are listed in Table IV. Of particular note is that the rate constants are uniformly an order of magnitude larger than those found when He or Ar is the collision partner with $I_2(v_E=0-2)$. The largest cross sections are for transfer to the β state, followed by the D' and D states, a trend similar to that found when Ar is the collision partner.[3,5] The large cross sections for electronic energy transfer are consistent with a model in which the attractive region of the intermolecular potential has a dominant role in determining the collision cross sections. The static electric polarizability of CF_4 is more than twice that of Ar,[30] so we expect a significantly enhanced interaction with ion-pair excited I_2. Akopyan *et al.* have explored the role that rare gas–I_2 complexes might play in the electronic relaxation of I_2 excited to the $f(0_g^+)$ ion-pair state,[31] while Stephenson *et al.* explored dissociation induced electronic relaxation in the NeICl van der Waals complex in the E ion-pair state 15 years ago.[32–34] It is possible that collision complexes of I_2 with CF_4 play a role in the rovibrational resonance effects that we observe. Formation of such complexes might result in selective excitation of internal degrees of freedom within CF_4 via an intramolecular vibrational redistribution (IVR) mechanism and would account for the large effective hard-sphere cross sections. Contradicting this conjecture is the observation of vibrational distributions in agreement with Franck-Condon factors, a result associated with sudden, impulsive interactions.[35] An examination of the dynamics of I_2-CF_4 van der Waals complexes would shed light on these intriguing issues.

TABLE IV. Total rate constants and hard-sphere collision cross sections for collisionally induced electronic energy transfer from the given initial state to the final electronic states D', β, and D.

Final state	Initial state $(v_E=0, J_E=23)$	$(v_E=0, J_E=55)$	$(v_E=1, J_E=55)$	$(v_E=2, J_E=55)$
	Energy transfer rate constants (10^{-16} m^3 s^{-1} $molecule^{-1}$)			
D'	1.56±0.15	2.28±0.17	2.5±0.2	2.5±0.2
β	2.57±0.17	2.71±0.16	3.1±0.2	3.1±0.2
D	0.36±0.03	1.10±0.08	1.28±0.08	1.42±0.12
	Hard-sphere collision cross sections ($Å^2$)			
D'	50±5	73±5	80±6	80±6
β	83±5	87±5	100±6	100±6
D	12±1	35±3	41±3	46±4

IV. CONCLUSION

In this report we have shown emission spectra and vibrational populations from the three lowest energy ion-pair states of I_2 populated through CF_4 collision-induced energy transfer from the E ion-pair state. Vibrational populations extracted from our spectral fits show a significant change from those found when either He or Ar was the collision partner. While the relative rate constants for transfer to the D', β, and D states differed between He and Ar collisions, the vibrational distributions within a particular electronic state are relatively independent of the identity of the collision partner. The data shown here show markedly different vibrational state distributions and significantly increased rate constants. We attribute these differences to the vastly increased number of pathways for CF_4 to accept the excess energy that accompanies the iodine electronic energy transfer, namely, rotational and vibrational degrees of freedom.

This article is copyrighted as indicated in the abstract. Reuse of AIP content is subject to the terms at: http://scitation.aip.org/termsconditions. Downloaded to IP: 130.58.65.10 On: Wed, 27 Nov 2013 21:36:19

Collisions with He or Ar most likely induce transitions to vibrational levels with both significant Franck-Condon overlap and small energy gaps with the initially prepared state, a trade-off that often produces a broad distribution in many vibrational levels. In the vibrational distributions shown here, we find that collisions with CF_4 are most likely to induce transitions to vibrational levels that maximize Franck-Condon overlap—a trend that tends to minimize the change in vibrational quantum number. We attribute the two low frequency bending modes of CF_4 to be particularly effective in accepting excess energy because of the associated energy gaps at the low v_E levels accessed here. Hence, the need to transfer large amounts of energy into relative translation with an atomic collision partner is lessened in a collision with CF_4, and it is far more likely to induce a transition to a vibronic level with good Franck-Condon overlap and a relatively large energy gap.

Of particular interest is the $E \rightarrow D$ electronic energy transfer in which we find evidence of specific, rotational level dependent, nonstatistical energy transfer that is resonant with the excitation of the ν_2 bending mode of CF_4 at 435 cm^{-1}. The excess rotational distribution in emission from the $v_D=0$ vibrational level that occurs after excitation to the state ($v_E=0$, $J_E=55$) but not after excitation to the state ($v_E=0$, $J_E=23$) is a strong evidence for such a process. In the former case there is sufficient energy from the $(v_E=0, J_E=55) \rightarrow (v_D=0, J_D=26)$ transfer to be resonant with the CF_4 $(0,1,0,0) \leftarrow (0,0,0,0)$ energy gap, while from the ($v_E=0$, $J_E=23$) state, there is insufficient energy to be resonant with any vibrational mode of CF_4 even when terminating at the state ($v_D=0$, $J_D=0$). However, regardless of any specific vibrational resonance effect, excitation of CF_4 internal degrees of freedom would explain the substantial propensity for populating the $v_D=0$ level after excitation to $v_E=0$, regardless of the I_2 rotational state involved. We find a similar mechanism in the $E \rightarrow D$ electronic energy transfer after excitation the states $v_E=1$ and $v_E=2$. However, the increased available energy when transferring the lowest two vibrational levels of the D state precludes an unambiguous identification of the specific CF_4 vibrational resonance involved.

Our analysis indicates a pronounced E-V collision-induced electronic energy transfer in the $I_2(v_E=0-2)+CF_4$ system. In the case of $E \rightarrow D'$ and $E \rightarrow \beta$ energy transfer, we only have indirect evidence of such through comparison of the vibrational state distribution in similar experiments in which He or Ar atoms are the collision partners. In comparing the $E \rightarrow D$ transfer from the initial states ($v_E=0$, $J_E=23$) and ($v_E=0$, $J_E=55$), however, we see specific evidence of excitation of the ν_2 bending mode of CF_4 as the available energy is increased above the threshold for excitation of this vibration. There exist many examples in the literature of vibrationally excited, electronic ground state, molecules inducing vibrational excitation in molecular collision partners.[36] Our data and that of Pravilov and co-workers[6,9] suggest that similar dynamics occur with ground state molecular collision partners and highly electronically excited I_2.

ACKNOWLEDGMENTS

This work has been supported by grants from the Camille and Henry Dreyfus Foundation and the Swarthmore College Faculty Research Fund.

[1] W. Ubachs, I. Aben, J. B. Milan, G. J. Somsen, A. G. Stuiver, and W. Hogervorst, Chem. Phys. **174**, 285 (1993).
[2] R. Teule, S. Stolte, and W. Ubachs, Laser Chem. **18**, 111 (1999).
[3] C. J. Fecko, M. A. Freedman, and T. A. Stephenson, J. Chem. Phys. **116**, 1361 (2002).
[4] C. J. Fecko, M. A. Freedman, and T. A. Stephenson, J. Chem. Phys. **115**, 4132 (2001).
[5] P. P. Chandra and T. A. Stephenson, J. Chem. Phys. **121**, 2985 (2004).
[6] M. E. Akopyan, N. K. Bibinov, D. B. Kokh, A. M. Pravilov, O. L. Sharova, and M. B. Stepanov, Chem. Phys. **263**, 459 (2001).
[7] M. E. Akopyan, N. K. Bibinov, D. B. Kokh, A. M. Pravilov, M. B. Stepanov, and O. S. Vasyutinskii, Chem. Phys. **242**, 263 (1999).
[8] N. K. Bibinov, O. L. Malinina, A. M. Pravilov, M. B. Stepanov, and A. A. Zakharova, Chem. Phys. **277**, 179 (2002).
[9] M. E. Akopyan, A. M. Pravilov, M. B. Stepanov, and A. A. Zakharova, Chem. Phys. **287**, 399 (2003).
[10] M. E. Akopyan, I. Y. Chinkova, T. V. Fedorova, S. A. Poretsky, and A. M. Pravilov, Chem. Phys. **302**, 61 (2004).
[11] M. E. Akopyan, I. Y. Novikova, S. A. Poretsky, A. M. Pravilov, A. G. Smolin, T. V. Tscherbul, and A. A. Buchachenko, J. Chem. Phys. **122**, 204318 (2005).
[12] T. V. Tscherbul, A. A. Buchachenko, M. E. Akopyan, S. A. Poretsky, A. M. Pravilov, and T. A. Stephenson, Phys. Chem. Chem. Phys. **6**, 3201 (2004).
[13] T. V. Tscherbul and A. A. Buchachenko, Chem. Phys. Lett. **370**, 563 (2003).
[14] J. C. D. Brand and A. R. Hoy, Appl. Spectrosc. Rev. **23**, 285 (1987).
[15] F. Martin, R. Basic, S. Churassy, and J. Verges, J. Mol. Spectrosc. **116**, 71 (1986).
[16] D. Cerny, R. Bacis, S. Churassy, D. Inard, M. Lamrini, and M. Nota, Chem. Phys. **216**, 207 (1997).
[17] D. R. T. Appadoo, R. J. Le Roy, P. F. Bernath, S. Gerstenkorn, P. Luc, J. Verges, J. Sinzelle, J. Chevillard, and Y. D'Aignaux, J. Chem. Phys. **104**, 903 (1996).
[18] P. Luc, J. Mol. Spectrosc. **80**, 41 (1980).
[19] S. Motohiro, S. Nakajima, and T. Ishiwata, J. Mol. Spectrosc. **212**, 194 (2002).
[20] J. P. Perrot, M. Broyer, J. Chevaleyre, and B. Femelat, J. Mol. Spectrosc. **98**, 161 (1983).
[21] T. Ishiwata and I. Tanaka, Laser Chem. **7**, 79 (1987).
[22] J. C. D. Brand, A. R. Hoy, A. K. Kalkar, and A. B. Yamashita, J. Mol. Spectrosc. **95**, 350 (1982).
[23] I. N. Levine, *Quantum Chemistry*, 4th ed. (Allyn and Bacon, Boston, 1991).
[24] R. J. Le Roy, University of Waterloo Chemical Physics Research Report No. CP-657R, 2004.
[25] T. A. Brunner and D. Pritchard, Adv. Chem. Phys. **50**, 589 (1982).
[26] J. E. Lolck, J. Raman Spectrosc. **11**, 294 (1981).
[27] T. Gabard, G. Pierre, and M. Takami, Mol. Phys. **85**, 735 (1995).
[28] P. Esherick, A. Owyoung, and C. W. Patterson, J. Mol. Spectrosc. **86**, 250 (1981).
[29] K. Lawley, P. Jewsbury, T. Ridley, P. Langridge-Smith, and R. Donovan, Mol. Phys. **75**, 811 (1992).
[30] *Handbook of Chemistry and Physics*, 87th ed., edited by D. R. Lide (CRC, Boca Raton, FL, 2006).
[31] M. E. Akopyan, I. Y. Novikova, S. A. Poretsky, and A. M. Pravilov, Chem. Phys. **310**, 287 (2005).
[32] T. A. Stephenson, Y. Hong, and M. I. Lester, Chem. Phys. Lett. **159**, 549 (1989).
[33] T. A. Stephenson, Y. Hong, and M. I. Lester, in *Dynamics of Polyatomic Van der Waals Complexes*, NATO Advanced Studies Institute, Series B: Physics, edited by N. Halberstadt and K. C. Janda (Plenum, New York, 1990), Vol. 227, p. 493.
[34] T. A. Stephenson, Y. Hong, and M. I. Lester, J. Chem. Phys. **94**, 4171 (1991).
[35] M. H. Alexander and G. C. Corey, J. Chem. Phys. **84**, 100 (1986).
[36] G. W. Flynn, C. S. Parmenter, and A. M. Wodtke, J. Phys. Chem. **100**, 12817 (1996).

This article is copyrighted as indicated in the abstract. Reuse of AIP content is subject to the terms at: http://scitation.aip.org/termsconditions. Downloaded to IP: 130.58.65.10 On: Wed, 27 Nov 2013 21:36:19